Supporting Information

Buckling Pneumatic Linear Actuators Inspired by Muscle

*Dian Yang, Mohit S. Verma, Ju-Hee So, Bobak Mosadegh, Christoph Keplinger, Benjamin Lee, Fatemeh Khashai, Elton Lossner, Zhigang Suo, and George M. Whitesides**

Fabrication of the VAMPs

The vacuum-actuated muscle-inspired pneumatic structures (VAMPs) were created by replica molding (Figure S1). We designed the molds using computer-aided design (CAD; Solidworks) and fabricated them in acrylonitrile butadiene styrene (ABS) plastic using a 3D printer (StrataSys Fortus 250mc). Curing a silicone-based elastomer (Ecoflex 00-30 or Elastosil) against the molds at room temperature (4 hours for Ecoflex 00-30 and 6 hours for Elastosil) produced separately, the two halves of the VAMPs. These two halves were aligned and bonded together by applying uncured elastomer at their interface, prior to placing them in an oven and curing at 60 °C for 15 minutes. A conical piece of the elastomer was bonded to the top of the actuator to provide additional material that allowed tubing (Intramedic polyethylene tubing, ID 0.76mm) to be securely attached to the structure. The conical piece was pierced by a cannula to allow tubing to be easily place into the VAMP. After the cannula was removed, the tubing is held in place and sealed from the atmosphere by elastic deformation of the conical piece of elastomer.

VAMPs that are capable of producing higher stresses (by using materials of higher modulus, $E \approx 2.5$ MPa) were made by directly 3D printing the pieces of the VAMPs using the Stratasys PolyJet 3D-printed (Objet Connex 500). The 3D printed pieces were then assembled by

gluing them with the URE-BOND® II urethane adhesive. The tubing was introduced with a cannula as in the case of VAMPs fabricated in Ecoflex or Elastosil.

Theoretical discussion of Young's modulus vs. stress output

Why the critical differential pressure (ΔP_{crit}) is proportional to Young's modulus at zero loading stress? We represent the elastomer using the neo-Hookean model.[1] Assuming the elastomer is incompressible, the model indicates that the stress-strain relation contains a single material constant—Young's modulus E. Let ΔP be the difference in the pressure between that in the ambient and that inside the actuator. In the absence of the applied load, the differential pressure ΔP relates to the actuation strain s by Equation S1.

$$\Delta P = Ef(s) \tag{S1}$$

This relation is obtained on the basis of dimensional considerations. The function $f(s)$ is nonlinear in strain, and depends on ratios of various geometric features (but is independent of the size of the features). If we make two actuators of identical geometric features, but of materials with different Young's moduli, we can plot $\Delta P/E$ as a function of s, and the two curves will fall on top of each other.

When $\Delta P/E$ is large, the cells in the actuator collapse, and the actuation strain reaches a plateau. The critical differential pressure ΔP_{crit} is reached when actuation strain approaches its maximum: $s_{\max} \approx 0.4$ (Figure 2A). Substituting $s = s_{\max}$ into Equation S1, we obtain a linear relationship between the critical differential pressure ΔP_{crit} and the Young's modulus E (Equation S2),

$$\Delta P_{\mathrm{crit}}/E = f(s_{\max}) = c, \tag{S2}$$

where c is a constant. The experimentally determined shape of the function $f(s)$ is given in Figure 2. Our experimental data show that $c \approx 0.025$.

Why the loading stress σ is proportional to Young's modulus at a fixed actuation strain?

Let σ be the nominal stress due to the hanging weight—that is, the weight T divided by the cross-sectional area of the undeformed actuator A. We regard an actuator as a thermodynamic system of two independent variables that can independently change the state of the actuator—the differential pressure and the loading stress. To a good approximation, the elastomer is incompressible. Hence, the state of the actuator depends on the differential pressure, but not on the absolute pressures inside and outside the actuator. Since the experiment is insensitive to small change in temperature, we do not list temperature as a variable. Using the neo-Hookean model, we may obtain Equation S3 on the basis of dimensional considerations:

$$s = g(\Delta P/E, \sigma/E), \tag{S3}$$

If we make two actuators with indistinguishable geometric features, but of materials with different Young's moduli, we can plot s as a function of $\Delta P/E$ and σ/E. The two surfaces will fall on top of each other.

When $\Delta P/E$ is large, the cells in the actuator collapse, and the actuation strain reaches a plateau. In this case, s becomes independent of $\Delta P/E$ and is only a function of σ/E (Equation S4). Therefore, at fixed actuation strain s^*, the relationship between the loading stress σ and Young's modulus is linear (Equation S5), where c^* is a constant depending on the value of s^*.

$$s = h(\sigma/E). \tag{S4}$$

$$\sigma/E = h^{-1}(s^*) = c^*, \tag{S5}$$

The behavior of VAMPs when one scales up (or down) the size of the geometric features

We have noted that one can obtain Equation S1 (i.e. $\Delta P = Ef(s)$) on the basis of dimensional considerations, where the function $f(s)$ is nonlinear in strain, and depends on ratios of various geometric features (but is independent of the size of the features). We, therefore, conclude that if we make two actuators of identical ratios of geometric features, but of different sizes of the geometric features, $\Delta P/E$ as a function of s will be identical for the two actuators. This subsequently means that the critical differential pressure ΔP_{crit} remains constant when one scales up or down the size of the geometric features of VAMPs, provided Young's modulus E stays constant.

We have further noted that one can obtain Equation S3 (i.e. $s = g(\Delta P/E, \sigma/E)$) on the basis of dimensional considerations, where the function $g(\Delta P/E, \sigma/E)$ depends on ratios of various geometric features (but is independent of the size of the features). We, therefore, conclude that if we make two actuators of identical ratios of geometric features, but of different sizes of the geometric features, s as a function of $\Delta P/E$ and σ/E will be identical for the two actuators. This subsequently means that the actuation strain s as a function of actuation stress σ at any differential pressure ΔP remains the *same* when one scales up or down the size of the geometric features of VAMPs, provided Young's modulus E stays constant. This is, in fact, a remarkable result. It means that one can be agnostic of the exact feature size of a VAMP, and obtain the same mechanical performance as long as the bulk dimensions of the VAMP are the same.

Loading stresses for VAMPs made of different elastomers

Figure 1C, D shows that VAMPs with indistinguishable geometrical sizes and shapes (34 mm × 28 mm × 46.5 mm) support higher maximum loads as the stiffness of the elastomer of which they are made increases (Movies S1 and S2).

A VAMP made of Ecoflex 00-30 (represented in Figure 1C, E = 43 kPa) supports a loading stress of about 0.5 kPa at 30% actuation strain, and a loading stress of about 1 kPa at 0% actuation strain. A VAMP made of Elastosil M4601 (represented in Figure 1D, E = 520 kPa) supports a loading stress of about 6 kPa at 30% actuation strain, and a loading stress of about 10 kPa at 0% actuation strain.

We have experimentally demonstrated up to 65 kPa loading stress with high stiffness materials (Stratasys PolyJet 3D printed soft material with a Young's modulus of $E \approx 2.5$ MPa, Figure S2). Figure S2 and Movie S3 show a VAMP that demonstrates ~65 kPa loading stress at 10% actuation strain when fabricated in a urethane elastomer with Young's modulus $E \approx 2.5$ MPa.

VAMPs made with higher moduli have the potential to generate even higher actuation stress at larger actuation strains (and, in principle, stress greater than 100 kPa under hyperbaric environments). Under normal atmospheric pressure, the theoretical maximum stress that a VAMP can generate is 100 kPa. This value can be reached with improvements in the design and fabrication.

The theoretical maximum actuation stress (i.e. atmospheric pressure 100 kPa) of the VAMP is the same as the maximum sustaining stress of human muscle (~100 kPa), and within a factor of four of the impulsive stress of human muscle (~350 kPa).[2] To reach a similar maximum force of muscle, machines with VAMPs can be made slightly bulkier to generate the

same force (i.e. arms with 3.5 times greater cross-sectional areas than those of an average human, which is an increase in the width of a factor of 1.87). In daily actions and in tasks such as assisted movement, humans do not ordinarily exert the maximum stress of their muscle. Thus, a VAMP should be able to realize most human-scale tasks; examples would include assistive devices for elderly, and systems for gentle manipulation of irregularly shaped objects such as fruit, or small animals. There is also the merit of safety that comes with having an artificial muscle that is slightly weaker than human muscle. VAMPs provide a good platform for developing robots that are collaborative, and potentially useful in settings such as hospitals, schools, or nursing homes.

Explanation for the increase of actuation strain at low stress

The anomalous increase of the actuation strain as a function of actuation stress is partially due to our definition of the actuation strain $s(\Delta P, \sigma)$. In Equation 3, $s(\Delta P, \sigma)$ is defined to be the ratio between the change in length of the actuator *after* loading, $L(\Delta P, \sigma) - L(0, \sigma)$, and the length of the actuator *before* loading, $L(0,0)$, which is a constant (note also that $L(\Delta P, \sigma) - L(0, \sigma) < 0$; this relationship means that the strain is always negative). Since our actuator is elastomeric, its length $L(0, \sigma)$ increases after the load is applied. On the other hand, increase in the length of the collapsed actuator after vacuum is applied $L(\Delta P, \sigma)$ is smaller, since the majority of the compliant elastomeric metastructure is compressed and consolidated. Therefore, the absolute value of the actuation strain $s(\Delta P, \sigma)$, at small actuation stress σ, is dominated by the behavior of $L(0, \sigma)$. At large actuation stress σ, the actuator is no longer capable of completely collapsing, and the decrease of $L(\Delta P, \sigma)$ with increase of actuation stress σ starts to dominate the behavior

of $s(\Delta P, \sigma)$. This decrease of $L(\Delta P, \sigma)$ gives rise to the shape for the rest of the curve (i.e. decrease in absolute value of the strain $s(\Delta P, \sigma)$ as a function of actuation stress σ).

Obtaining the Young's moduli of different elastomers

The Young's moduli of the elastomers were measured with standard dog-bone shaped samples in an Instron 5566. The samples were stretched at a strain rate of 0.5 mm/s until rupture. The modulus was estimated by linear fitting of the stress-strain data from 0 to 66% strain, which was within the linear regime. The slope of this fitting was extracted as an estimate for Young's modulus.

Specifications for the "arm-like" structure

We estimated the force required to lift the lower part of the skeleton (10 kN) based on Equation S5, given the cross-sectional dimensions of the VAMP (50 mm × 40 mm), and the material (Elastosil) required to generate this force. The VAMP was 240 mm long so that the "arm" could achieve the required range of movement (i.e. the total dimension is: 50 mm × 40 mm × 240 mm). Metal wires in rubber tubing served as tendons to connect the VAMP to the skeleton.

Measurement of thermodynamic efficiency

We generated the pressure-volume hysteresis curves by pumping water (an incompressible fluid) in and out of the actuator. The actuator was fully submerged in a 1-gallon container of water. The hydraulic actuation, and measurement of volume was performed with a syringe pump (Harvard Apparatus, PHD 2000), and the pressure measurement was performed with a pressure sensor (Transducers Direct, TDH31) connected to the syringe pump and the pressure transfer line

(Figure S3). We clamped the actuator in a position that was submerged fully in water. We filled the actuators with water by submerging them in the container of water and deflating them several times until bubbles no longer emerged.

Within each test, we switched from deflation to inflation when the actuator had achieved ~20% contraction. We chose the rate of deflation and inflation to be 0.081 mL/s, which was sufficiently slow to achieve quasistatic conditions. We repeated the deflation-inflation cycle six times.

Since the fluid used for inflation/deflation (water) is effectively incompressible, we could equate the volume decrease/increase of fluid in the syringe to that of the increase/decrease in the volume of the channels in the VAMPs. The VAMPs required removal of $V_0 = 16.6$ mL of water to achieve ~20% actuation, lifting a 500-g test weight by a height of $\Delta h = 8.9\ mm$, while the applied differential pressure ramped up from 0 kPa to 18 kPa. We calculated the thermodynamic efficiency η by dividing "energy out" E_{out} by "energy in" E_{in} (Equation S6). E_{out} was obtained by calculating the potential energy gain of lifting the weight ($m = 500$ g was the weight we used, and g is the gravitational constant) (Equation S7). E_{in} was obtained by integrating the differential pressure with respect to the change in volume (Equation S8). This value is represented by the area under the P-V curve (Figure S3B).

$$\eta = E_{\text{out}}/E_{\text{in}}. \tag{S6}$$

$$E_{\text{out}} = mg\Delta h. \tag{S7}$$

$$E_{\text{in}} = \int_0^{V_0} P(V)\, dV. \tag{S8}$$

Over a total of six runs, we obtained an efficiency of $\eta = 27.2\% \pm 0.6\%$. Note that the loss of energy due to hysteresis was small compared to the work done by the syringe pump

during actuation (Figure S3). The loss of efficiency was mainly due to the storage of elastic energy in the elastomer, with a small contribution from hysteresis.

Thermodynamic efficiency of this type of actuator (which combines vacuum and collapsing of an elastomeric structure) can be improved through better engineering, with the potential to reach 40% or higher. The main loss in efficiency is due to the elastic energy absorbed and dissipated as heat while collapsing the elastomeric structure consisting of beams. In principle, one can engineer a better structure (perhaps with smaller beams, or beams fabricated in a mixture of materials with different moduli) that produces less stress while compressed, while providing the same structural rigidity (under the same load) in the direction perpendicular to the intended direction of actuation. One can also use materials that are closer to perfectly elastic (that is, they demonstrate little viscoelasticity) to improve the efficiency of VAMPs further.

Measurement of lifetime

We measured the lifetime of three VAMPs fabricated in Elastosil by connecting them to an Arduino-controlled/gated pneumatic source. The VAMPs were each fully deflated and then re-inflated to the initial state repeatedly. The VAMPs were actuated at a frequency of 1Hz, and left running continuously for ~12 days. This interval resulted in more than 1,000,000 cycles of actuation. We tested the loading stress vs. actuation strain of these three VAMPs, and observed no significant change in the curves (Figure S5).

VAMPs have a potential for long lifetime for two reasons: i) the use of a single material of fabrication allows them to be made into a single piece, and thus to have no seams or regions of concentrated stress; ii) the maximum strain occurring in the elastomers is also moderate in VAMPs and less than that in positive pressure systems subjected to inflation. Since the lifetime

of elastomers in use usually correlates positively with strain,[1] VAMPs will have longer lifetimes than systems that operate at positive pressure and at higher strains.

Speed of actuation of VAMPs

VAMPs demonstrate moderately rapid actuation. Complete actuation of the structures shown in Figure 1 using a pneumatic pressure line with a 0.75 mm inner diameter and 10 cm length takes ~1 second (this speed is far from optimized). The shear friction between the air and the tubing is the primary factor that limits actuation speed and thus, this speed is governed by the diameter of the pneumatic port. Hagen–Poiseuille equation determines that the volumetric flow speed Q of a fluid through a tube (approximated as a cylindrical pipe with laminar flows) is proportional to r^4, where r is the radius of the tube (Equation S9).

$$\Delta P = \frac{8\mu L Q}{\pi r^4}. \qquad \text{(S9)}$$

Here, ΔP is the pressure drop along the tube, L is the length of the tube, and μ is the viscosity of the fluid.

Therefore, VAMPs with wider pneumatic tubing can drastically increase the speed of the actuator. In our "arm-like" structure, the VAMP with a pneumatic port radius of 3 mm is able to generate very fast motions (in Figure 3 and Movies S4 and S5, lifting the arm takes 0.5 s and lifting a volleyball takes 0.6 s). We compared this speed to the best speed of a young male researcher (in Figure S5 and Movies S6 and S7, lifting the arm takes 0.17 s and lifting a volleyball takes 0.2 s); the VAMP only takes three times longer. This is an impressive value considering that the speed of this particular VAMP system is still far from optimized, as explained by Equation S9. Further increase in the speed of the "arm-mimetic" structure is possible (and potentially to a speed faster than that of human arms), but it will likely involve

improved lubrication of the arm joint, and a vacuum source/pump with a pneumatic port of larger radius—neither are scientifically challenging tasks.

Relationship between stress and strain for VAMPs under passive loading and elastic energy storage of VAMPs

We characterized the relationship between stress and strain (or force and length) for seven different VAMPs when loaded with weights passively (Figure S7). The relationship is linear under a positive loading. This relationship demonstrates that VAMPs are capable of elastic energy storage under tension—energy can be returned as the work done by the passive force as VAMPs elastically recover. This relationship also shows that VAMPs are compliant—a natural consequence of them being made of elastomers; this compliance/elasticity will allow VAMPs to absorb shock and perform non-damaging interactions with the environment.

To obtain the relationship between stress and strain under negative loading, one can approximate it by using the applied differential pressure vs. strain data in Figure 2A, B, and taking the applied differential pressure as the negative loading. This approximation is valid, because applying a differential pressure to the bottom surface of the VAMP is physically equivalent to applying a stress to the surface externally. We used this approximation to obtain the complete passive loading curve in Figure S8B.

A mechanical model for VAMPs

We have constructed a model of VAMPs that includes three levels: 1) A simplified model (Figure S8A, left)—consisting of a passive element and a contractile element in parallel—describes the overall behavior of the system, and is comparable to the Hill model of muscle.[3]

Here, the passive element acts as a spring and resists the action of actuation, while the contractile element generates a direct driving force. 2) A more complex mechanical model explains how the structure and material properties govern the contractile element and the passive element (Figure S8A, right). Here, the elastic repulsion force from the system of beams is modeled as a passive spring; the outer surface of the actuator, which contracts linearly under a differential pressure, is modeled as an active piston. The tubing that connects the actuator to the vacuum source is modeled as a cylindrical pipe with laminar flow. 3) An analytical model demonstrates that the structural model can provide a system of equations to generate a control model, with explicit formulas (Equation S16); the actuation distance as a function of time $x(t)$ can be solved via a differential equation, given the differential pressure that drives the actuators.

We define force F_{PE} to be the force generated by the passive element (PE) of a VAMP. The force F_{PE} points downwards when the VAMP is compressed. F_{PE} was measured in a passive loading condition and plotted in Figure S8B in red. We note that F_{PE} is linear for the majority of the positive and negative range of the VAMP, and diverges when the VAMP reaches the minimum length (when all the beams are collapsed together). We can thus proximate F_{PE} with Equation S10, while x is less than the maximum contraction length of the VAMP.

$$F_{PE} = kx, \text{if x} < \text{x}_{max} \tag{S10}$$

When x equals to the maximum contraction length of the VAMP, we can proximate F_{PE} with:

$$F_{PE} = +\infty, \text{if x} = \text{x}_{max} \tag{S11}$$

The passive element F_{PE} effectively acts like a spring with a stopper.

We now obtain the force F_{CE} generated by the contractile element (CE) of a VAMP. Due to the arrangement of the beam structures, the motion of the VAMP is restricted only to the direction of actuation, and is driven like a piston by the pressure difference between inside and

outside the VAMP. Let P_{atm} be the atmospheric pressure, or pressure outside the VAMP, P_{in} be the pressure inside the VAMP, and P_{source} be the pressure applied by the vacuum source. Let m be the load carried by the VAMP, and A be the cross-sectional area of the VAMP. Looking at the bottom surface, we may write Equations S12 and S13:

$$F_{CE} = (P_{atm} - P_{in})A \tag{S12}$$

$$F_{total} = F_{CE} - F_{PE} = mg + m\ddot{x} \tag{S13}$$

Finally, we obtain the dissipative force from the tubing. Looking at the tubing that transduces the pressure to the VAMP (and approximating the tubing as a cylindrical pipe with laminar flow), we may write the corresponding Hagen–Poiseuille equation:

$$P_{in} - P_{source} = \alpha Q = \alpha V\dot{x} \tag{S14}$$

where $\alpha = \frac{8\mu L}{\pi r^4}$ is a constant.

Plug in Equation S14 into S12 for P_{in}, and then S12, S10 into S13 for F_{CE}, F_{PE}, we have:

$$(P_{atm} - P_{source})A = mg + kx + \alpha A^2\dot{x} + m\ddot{x} \tag{S15}$$

Notice that $\Delta P = P_{atm} - P_{source}$ is the nominal differential pressure we applied to the VAMP and write $\beta = \alpha A^2 = \frac{8\mu L A^2}{\pi r^4}$ as a new constant, we obtain a simplified version of Equation S15:

$$\Delta P * A = mg + kx + \beta\dot{x} + m\ddot{x} \tag{S16}$$

Equation S16 is the governing equation of a VAMP driven by the differential pressure ΔP, and constitutes a control model for a VAMP.

To do some simple analysis, we see that in quasi-static conditions, the equation simplifies to

$$\Delta P * A = mg + kx, \tag{S17}$$

which states a simple balance of force: the pressure applied across the bottom membrane of VAMP ($\Delta P * A$) must balance the weight sustained (mg) and the spring-like elastic force of the

beam system kx. In a dynamic condition, the driving force ($\Delta P * A$) must also provide the acceleration for the mass ($m\ddot{x}$), as well as overcome the air frictional-resistance of the pneumatic input line ($\beta\dot{x}$).

Dynamic measurements of VAMPs

We used a high-speed camera (Vision Research Inc. Phantom v7.3) to capture and measure the dynamic behaviors of the large VAMP used in the "arm-like" structure (fabricated in Elastosil, with dimension 50 mm × 40 mm × 240 mm) at 100 frames per second. We measured the position of the bottom surface the VAMP using the Prewitt horizontal edge-finding algorithm in Mathworks® Matlab, and calculated its velocity and acceleration. We applied a smoothing algorithm by averaging results from seven neighboring frames to eliminate some of the noise resulting from the edge-finding process. The resulting displacement, velocity, and acceleration curves are consistent with our control model (the curves are shown in Figure S9, and the setup is shown in Movie S12).

We used the same high-speed camera to capture and measure the dynamic behaviors of the smaller VAMPs (fabricated in Elastosil, with dimension 34 mm × 28 mm × 46.5 mm) used in dynamic characterization. The displacement, velocity, and acceleration curves (Figure S10) were obtained using the same method as described previously. We measured the VAMP three times in this characterization, while adjusting the loading stress by using different weights.

Comparing the dynamic characteristics of VAMPs to biological muscle

We can compare the relationship between force and velocity for VAMPs to that of a vertebrate muscle. A frog muscle demonstrates a stress of 250 kPa at a strain rate of 0 s^{-1} and a

stress of 0 kPa at a strain rate of 2 s^{-1}.[4] In Figure S10, we show that VAMPs made of Elastosil demonstrate a stress of 10 kPa at a strain rate of 0.5 s^{-1} and a stress of 0 kPa at a strain rate of 4 s^{-1}. As shown in the main text, the actuation stress of VAMPs is proportional to the stiffness of the material the VAMPs is made of, up to critical Young's modulus (E ≈ 5 MPa). Hence we project that VAMPs made using materials with a critical Young's modulus, that is 10 times stiffer than that used here, will have a peak stress of 100 kPa at a strain rate of 0.5 s^{-1}. The strain rate at no load of VAMPs (4 s^{-1}) compares well to that of a frog muscle (2 s^{-1}). But as shown in Figure S5, the current iteration is slower than that of a warmer human muscle. The maximum shortening speed for natural skeletal muscles ranges from <1 s^{-1} to 20 s^{-1}[5]. As explained in the section "Speed of actuation of VAMPs," however, we know that the speed of VAMPs demonstrated here does not represent a physical limitation, and can be largely improved using tubing and vacuum ports of larger radii.

Comparison of VAMPs to biological muscle, engineering actuators, and "muscle-like" actuators

A comparison of the performance of VAMPs to that of various engineering actuators is provided in Table S1 (data in Table S1 are extracted from a review on mechanical actuators[6] and a review on artificial muscles[2]). It shows that VAMPs closely resemble the properties of muscle and even though they are not as strong as some hard actuators such as pneumatic pistons and hydraulic pistons, they have additional features such as compliance, shock absorbance, elastic energy storage, no volume expansion during actuation, and self-sealing/repairing when punctured.

We compare the performance of VAMPs to that of other potentially "muscle-like"

actuators in Table S2 (data in Table S2 are extracted from reviews[2, 6-8], and original studies[9, 10]). We note that VAMPs perform similarly (on the same order of magnitude) to muscle in actuation strain, actuation stress, power density, and efficiency. Dielectric elastomer (DE) actuators outperform muscle and VAMPs in actuation stress, actuation strain, and maximum efficiency, but they suffer from dielectric breakdowns and require high voltages for operation. Although McKibben actuators outperform muscle and VAMPs in actuation stress, actuation strain, and power density, the elastomeric nature of VAMPs offers unique advantages over McKibben actuators and provides additional features, as discussed previously. Future improvement in design and materials will allow VAMPs to further enhance their performance.

The advantage of non-expansion of VAMPs compared to McKibben actuator

VAMPs do not expand in radius when actuated, and thus can function in space-limited environments. To quantify how much space can be saved, we compare VAMPs to the state-of-the-art pneumatic artificial muscle—the McKibben actuator. A McKibben actuator starts as a cylinder when un-actuated, and expands close to a pumpkin shape at full actuation strain (and under small or moderate load, such as <100 kPa—the range VAMPs operate at), where the pleat takes the shape of a half circle[8]. We take a typical radius to length ratio (for the un-actuated cylindrical state) of McKibben actuator: $R/L = 0.125$, where R = 1.25 cm and L = 10 cm. At full actuation, the widest part of the actuator has radius:

$$R' = R + {L}/{\pi} \simeq 1.25\ cm + {10\ cm}/{3.1416} = 4.43\ cm, \qquad \text{(S17)}$$

giving an increase in radius of ${L}/{R\pi} = 255\%$. By contrast, VAMPs experience no expansion in volume under actuation at any load. Thus all 255% of radius expansion is saved.

Characterizing the drift of VAMPs while holding a position

VAMPs are excellent in holding intermediate positions. An example of a demonstration of ability is the measurement conducted in the measurement of thermodynamic efficiency. As described in the SI section "Measurement of thermodynamic efficiency", the P-V in Figure S3B is measured by very slowly actuating a VAMP from 0% strain to 20% strain (over the course of 3 minutes) in quasi-static condition. The VAMP in this measurement demonstrates the ability to hold position at any position between 0% strain to 20% strain, given the control of volume ΔV. The actuator also exhibits no significant drift—the change in strain of a VAMP shown in Figure 1D is less than 1% of the height lifted at 20% strain, under a load of 500 g, over a period of 10 minutes, tested in the setup shown in Figure S3A. We speculate that the drift comes mostly from leakage in the couplings of tubes.

Methods for repairing VAMPs after damage

There are many ways one can potentially temporarily repair damage of an elastomeric actuator. Figure S6 and Movie S11 demonstrate that the structure can resist small punctures, without the need of immediate repair. Applying silicone glue (such as Sil-Poxy® from Smooth-On Inc.) to the damaged site can achieve more permanent patching (for actuators made of silicone polymers) or patching larger points of entry to re-establish pneumatic enclosure. If parts of the actuator are sufficiently damaged that they cannot buckle properly, they can in principle be completely fixated by applying larger quantities of silicone glue to the damaged area; the cellular structure allows the remaining part of the actuator still to function properly.

SI References

[1] A. N. Gent, *Engineering with Rubber: How to Design Rubber Components*, Carl Hanser Verlag GmbH Co KG: München, Germany, **2012**.

[2] J. D. Madden, N. A. Vandesteeg, P. A. Anquetil, P. G. Madden, A. Takshi, R. Z. Pytel, S. R. Lafontaine, P. A. Wieringa, I. W. Hunter, *IEEE J. Ocean. Eng.* **2004**, *29*, 706.

[3] A. Hill, *Proc. R. Soc. London, B* **1938**, *126*, 136.

[4] K. Edman, *J. Physiol.* **1988**, *404*, 301.

[5] R. Josephson, *Annu. Rev. Physiol.* **1993**, *55*, 527.

[6] J. Huber, N. Fleck, M. Ashby, "The Selection of Mechanical Actuators Based on Performance Indices", presented at *Proc. R. Soc. London, A*, 1997.

[7] P. Brochu, Q. Pei, *Macromol. Rapid Commun.* **2010**, *31*, 10.

[8] F. Daerden, D. Lefeber, *Eur. J. Mech. Environ. Eng.* **2002**, *47*, 11.

[9] M. D. Lima, N. Li, M. J. De Andrade, S. Fang, J. Oh, G. M. Spinks, M. E. Kozlov, C. S. Haines, D. Suh, J. Foroughi, *Science* **2012**, *338*, 928.

[10] C. S. Haines, M. D. Lima, N. Li, G. M. Spinks, J. Foroughi, J. D. Madden, S. H. Kim, S. Fang, M. J. de Andrade, F. Göktepe, *Science* **2014**, *343*, 868.

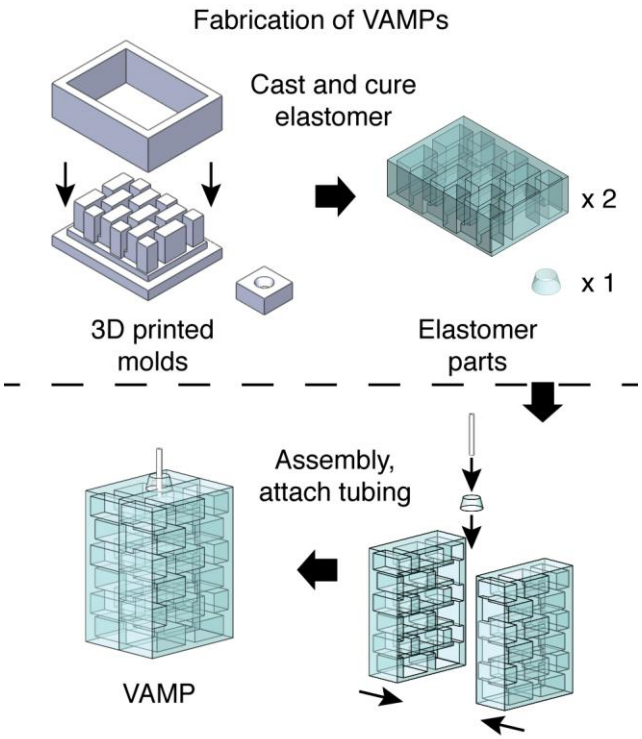

Figure S1. Steps involved in the fabrication of VAMPs.

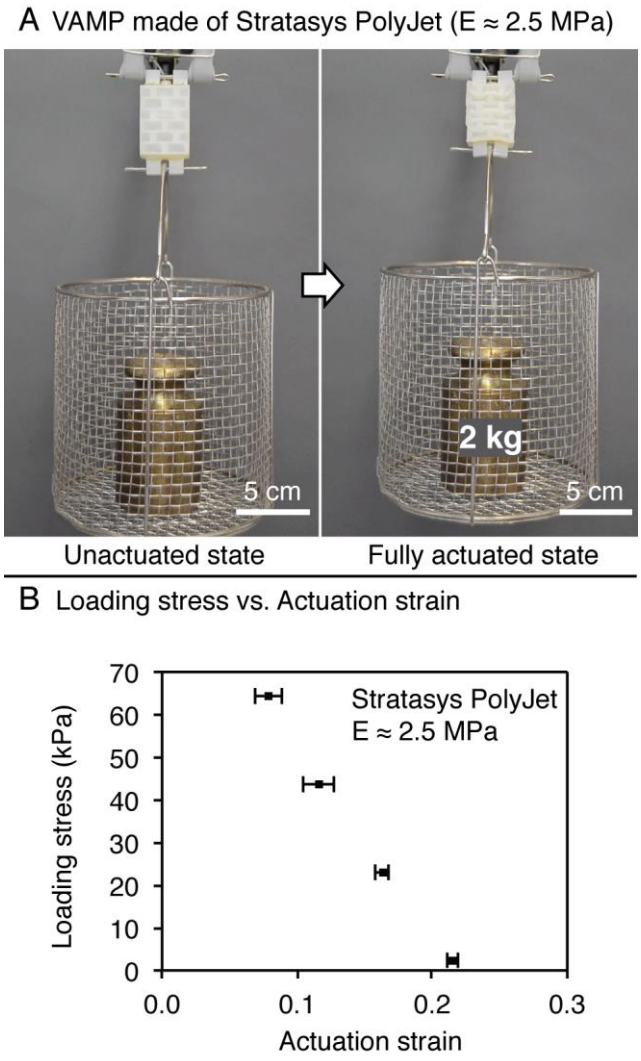

Figure S2. Demonstration of stress generated by a VAMP made from a high stiffness material (Stratasys PolyJet 3D printed material). (**A**) A VAMP of the same geometry as in Figure 1 (34 mm × 28 mm × 46.5 mm), but fabricated in Stratasys PolyJet 3D printed material (E ≈ 2.5 MPa at 66% strain) lifts a heavier weight (2 kg). See Movie S3 for the video. (**B**) Loading stress as a function of actuation strain for VAMPs fabricated in Stratasys PolyJet 3D printed material. The applied differential pressure is set to $\Delta P = 90$ kPa.

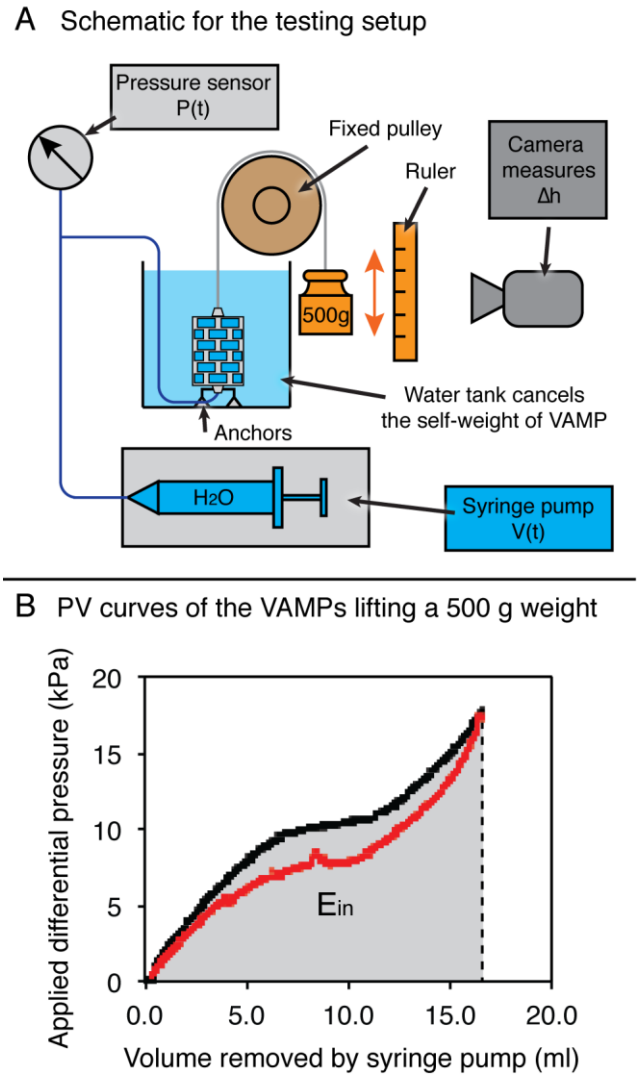

Figure S3. Experiment used to determine the thermodynamic efficiency of operation of a VAMP. (**A**) Schematic describing the setup used for testing. (**B**) P-V curves of a VAMPs fabricated in Elastosil lifting a 500 g weight. The actuation curve is marked in black, and the return curve is marked in red. The shaded area $\boldsymbol{E_{in}}$ represents the fluidic energy input via the syringe pump.

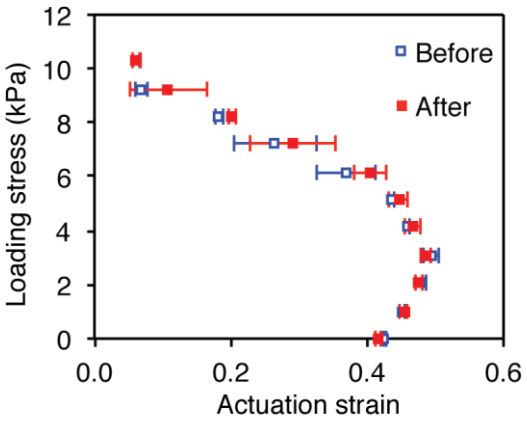

Figure S4. Comparison of the loading stress vs. actuation strain curve of VAMPs (fabricated in Elastosil, 34 mm × 28 mm × 46.5 mm) before and after 1,000,000 cycles of actuation at 1Hz. Reported values are mean ± S.D. (n = 3 different samples).

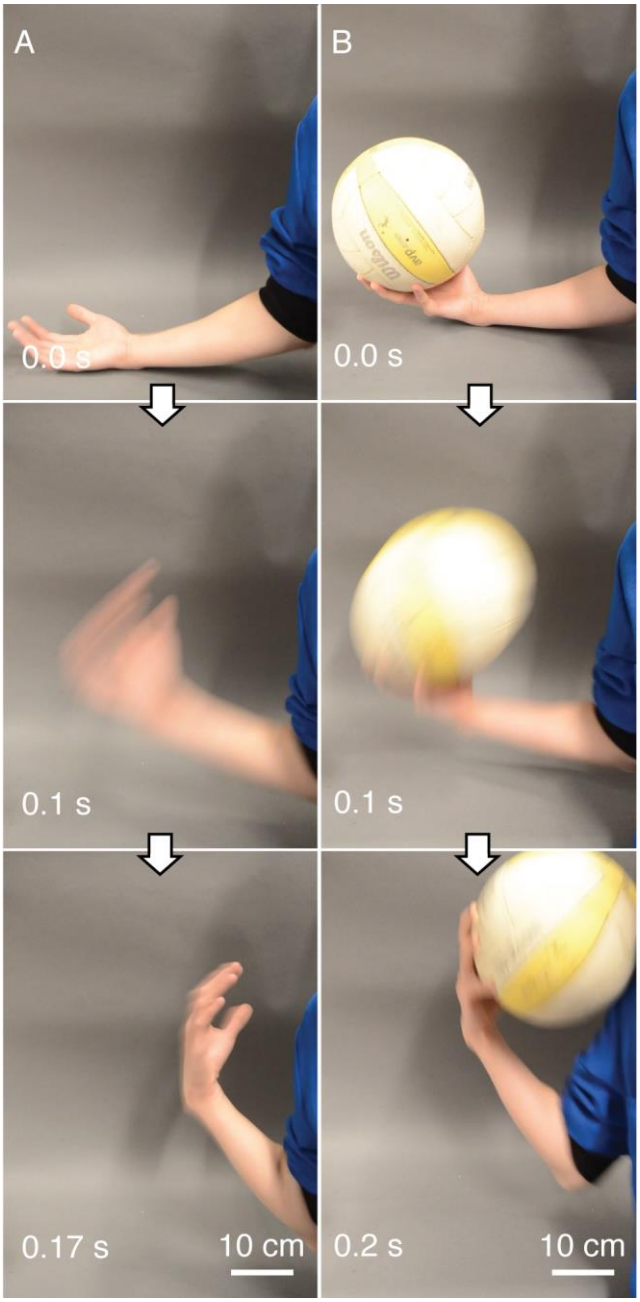

Figure S5. Speed of actuation of a human arm for quantitative comparison with VAMPs. (**A**) A human arm of a young male researcher contracting as rapidly as possible. (**B**) A human arm of a young male researcher contracting as rapidly as possible, while lifting a volleyball, which has a standard size and weighs 274 g. See Movies S6 and S7 for the videos.

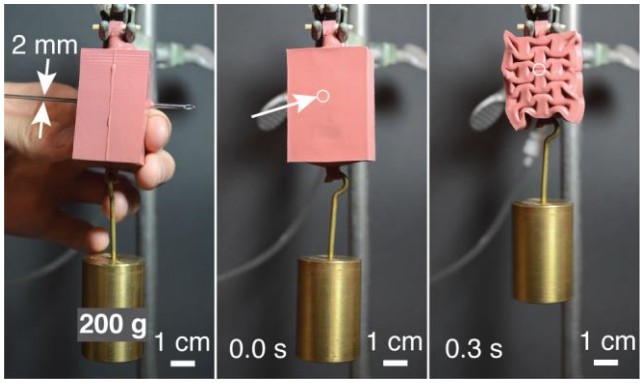

Figure S6. Self-sealing preserves performance after puncture. A VAMP is punctured by a 2 mm thick cannula. No visible change to the contractile function was observed. See Movie S11 for the video.

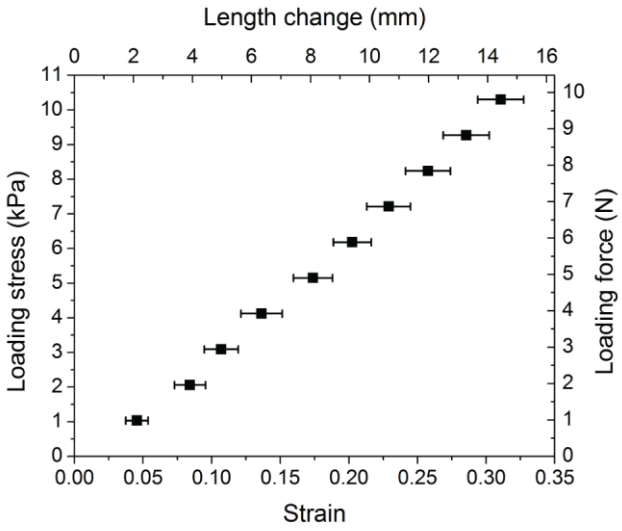

Figure S7. The relationship between stress and strain for VAMPs (fabricated in Elastosil, 34 mm × 28 mm × 46.5 mm) under passive loading. Reported values are mean ± S.D. (n = 7 different samples).

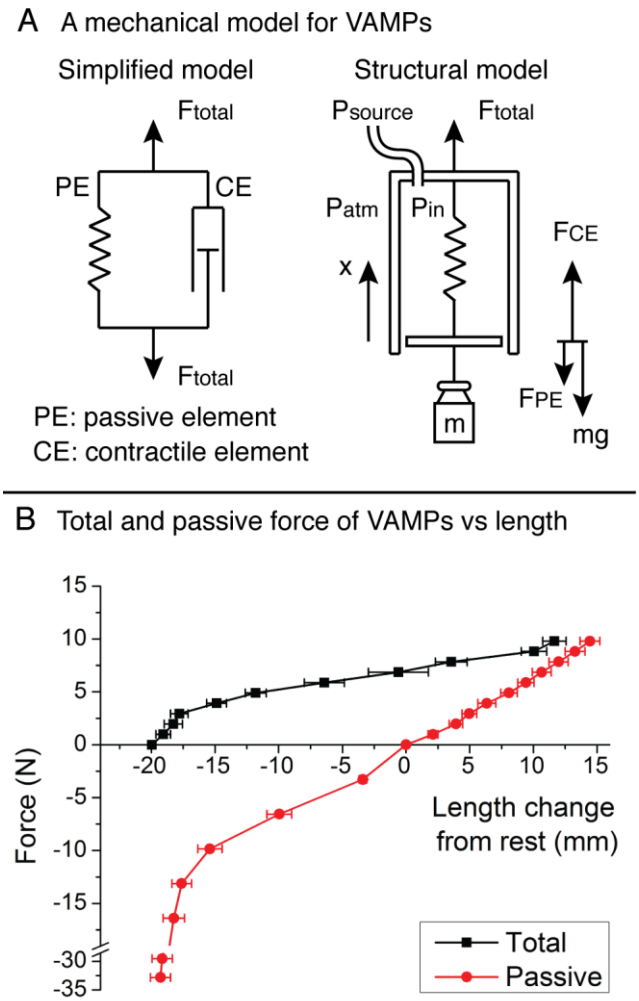

Figure S8. A mechanical model for VAMPs that resembles the Hill's model for muscle. (A) Two diagrams showing: 1) a simplified model that illustrates the force elements in a VAMP, and 2) a more detailed structural model that captures and simplifies the complex inner-structures of a VAMP. **(B)** The total (passive + active) and passive forces of VAMPs (fabricated in Elastosil, 34 mm × 28 mm × 46.5 mm) vs. the length change from the rest position. Reported values are mean ± S.D. (n = 7 different samples).

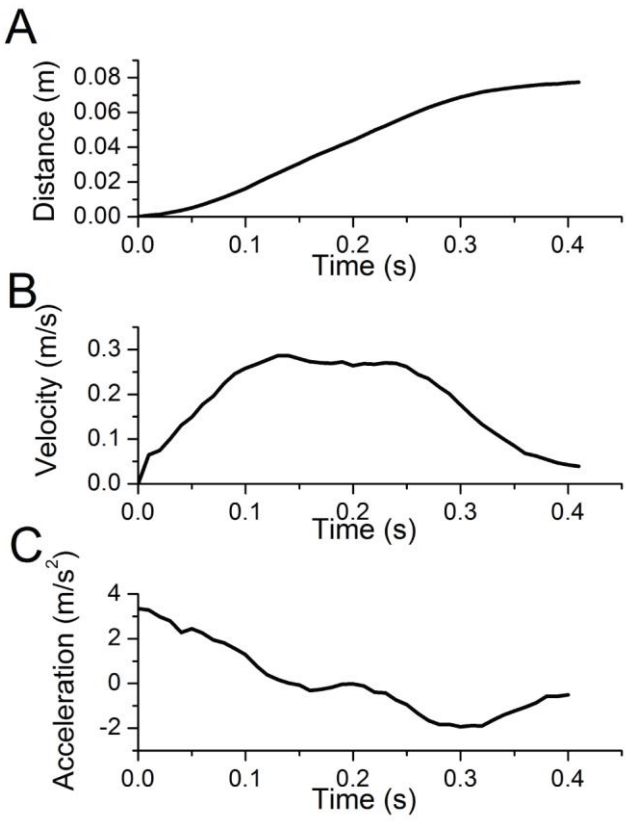

Figure S9. Dynamic measurements of the VAMP (fabricated in Elastosil, 50 mm × 40 mm × 240 mm) in the "arm-like" structure with a 500 g-weight (See Movie S12 for video). **(A)** The vertical displacement of the weight lifted by the VAMP as a function of time. **(B)** The velocity of the weight as a function of time, obtained by taking the time derivative of the displacement. **(C)** The acceleration of the weight as a function of time, obtained by taking the time derivative of the velocity.

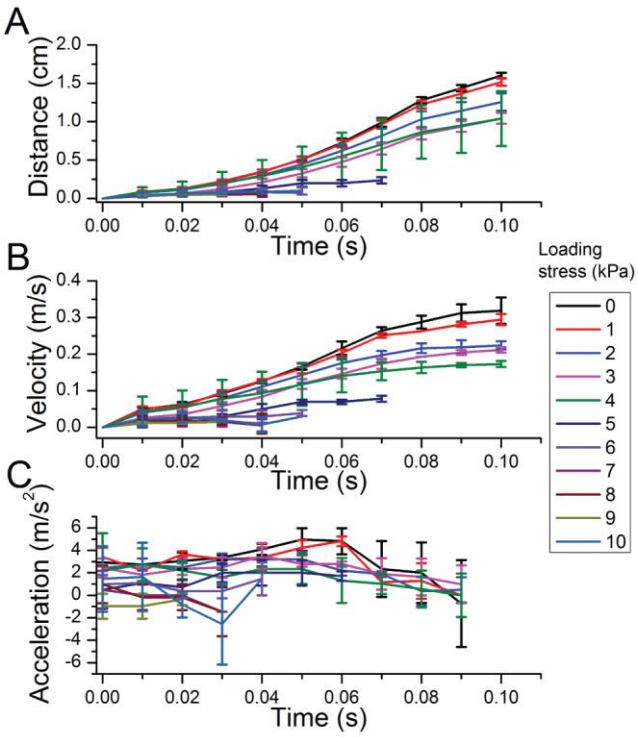

Figure S10. Dynamic measurements of a VAMP (fabricated in Elastosil, 34 mm × 28 mm × 46.5 mm) under different loading conditions. Reported values are mean ± S.D. (n = 3 measurements). **(A)** The vertical displacements of various weights lifted by the VAMP as functions of time. **(B)** The velocities of the weights as functions of time, obtained by taking the time derivatives of the displacements. **(C)** The accelerations of the weights as functions of time, obtained by taking the time derivatives of the velocities.

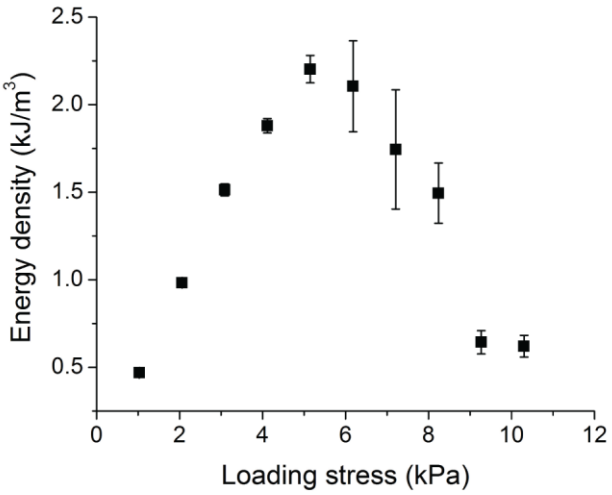

Figure S11. The relationship between energy density and loading stress σ for VAMPs (fabricated in Elastosil, 34 mm × 28 mm × 46.5 mm), derived from the relationship between force and length for VAMPs. Reported values are mean ± S.D. (n = 7 different samples).

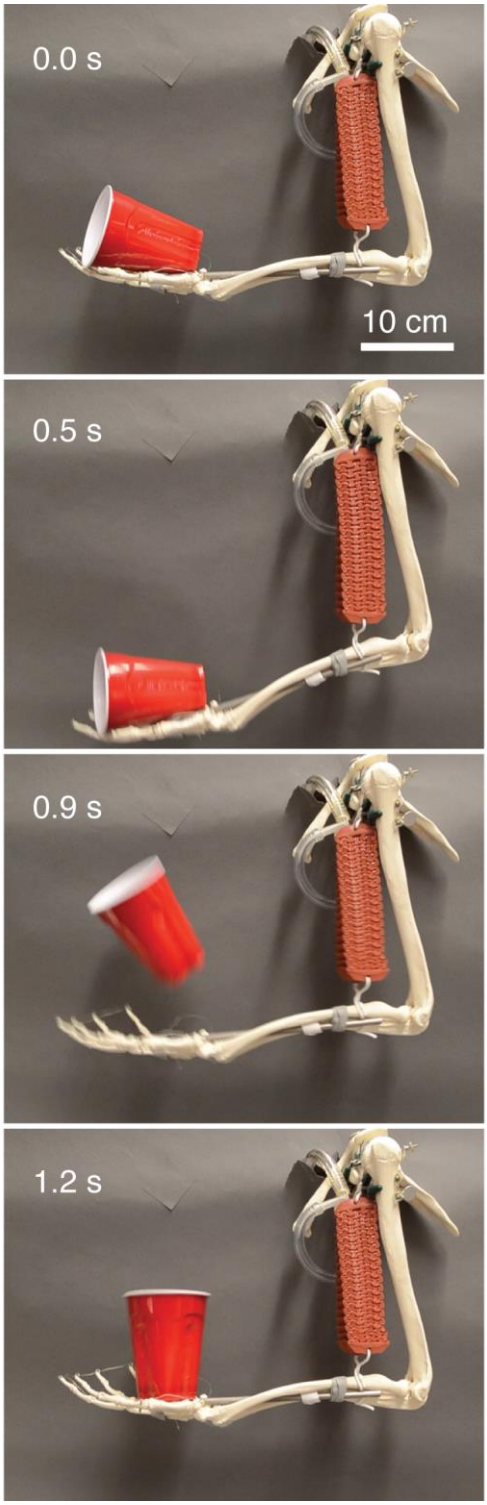

Figure S12. The "arm-like" structure can perform dynamic tasks, such as flipping a cup in the palm of its "hand" into an upright position. Scale bars are 10-cm long. Also see Movie S8.

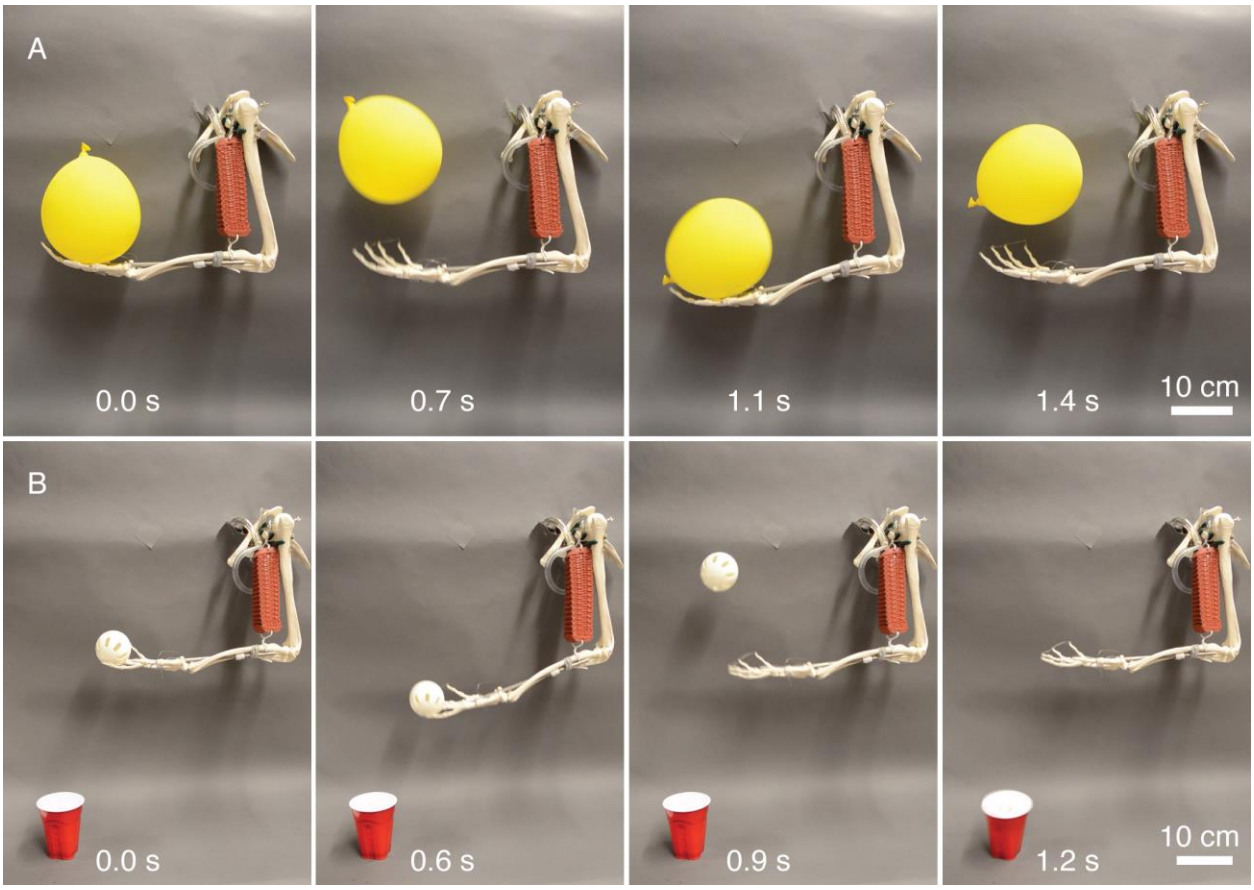

Figure S13. More demonstrations of the "arm-like" structure driven by VAMPs while performing muscle-like tasks. (**A**) Throwing and catching a balloon. (**B**) Throwing a ball into a cup without knocking over the cup. Scale bars are 10-cm long. Also see Movies S9 and S10.

Table S1. Comparisons of VAMPs to biological muscle and engineering actuators. Data in Table S1 are extracted from a review on mechanical actuators[6] and a review on artificial muscle.[2]

Actuator type	Maximum actuation strain	Maximum actuation stress (MPa)	Maximum power density (W/m^3)	Density (kg/m^3)	Efficiency
Low strain piezoelectric	5×10^{-6}-3×10^{-5}	1-3	1×10^{8}-1×10^{9}	2600-4700	> 0.9999
High strain piezoelectric	5×10^{-5}-2×10^{-4}	4-9	9×10^{7}-5×10^{8}	7500-7800	0.90-0.99
Piezoelectric polymer	2×10^{-4}-1×10^{-3}	0.5-5	≈ 3×10^{8}	1750-1900	0.90-0.95
Thermal expansion (10 K)	9×10^{-5}-3×10^{-4}	20-50	≈ 6×10^{4}	3900-7800	2×10^{-5}-3×10^{-4}
Thermal expansion (100 K)	9×10^{-4}-3×10^{-3}	200-500	≈ 6×10^{6}	3900-7800	2×10^{-4}-3×10^{-3}
Magneto-strictor	6×10^{-4}-2×10^{-3}	90-200	1×10^{8}-7×10^{8}	6500-9100	0.80-0.99
Shape memory alloy	7×10^{-3}-7×10^{-2}	100-700	7×10^{5}-1×10^{8}	6400-6600	0.01-0.02
Moving coil transducer	1×10^{-2}-1×10^{-1}	4×10^{-3}-5×10^{2}	5×10^{5}-2×10^{6}	7000-7600	0.50-0.80
Solenoid	0.1-0.4	4×10^{-2}-1×10^{-1}	1×10^{4}-4×10^{4}	3800-4400	0.50-0.80
VAMPs	≈ 0.4	≈ 0.1	> 1×10^{5}	≈ 500	≈ 0.27
Muscle	0.2-0.4	0.1-0.35	5×10^{4}-3×10^{5}	1000-1100	≈ 0.4
Pneumatic	0.1-1	0.5-0.9	≈ 5×10^{6}	180-250	0.30-0.40
Hydraulic	0.1-1	20-70	≈ 5×10^{8}	1600-2000	0.90-0.98

Table S2. Comparisons of VAMPs to biological muscle and other various "muscle-like" actuators. Data in Table S2 are extracted from reviews,[2, 6-8] and original studies.[9, 10]

"Muscle-like" actuators	Maximum actuation strain	Maximum actuation stress (MPa)	Maximum power density (W/kg)	Efficiency	Reference
DE actuators	≈ 0.8[a)]	3-7	4×10^{2}-5×10^{3}	0.6-0.9	(6,7)
Twisted CNT yarn	≈ 0.07	≈ 80	≈ 3×10^{4}	≈ 5×10^{-3}	(9)
Twisted fish line	≈ 0.35	≈ 80	≈ 3×10^{4}	≈ 1×10^{-2}	(10)
VAMPs	≈ 0.4	≈ 0.1	>2×10^{2}	≈ 0.27	Current work
Muscle	0.2-0.4	0.1-0.35	5×10^{1}-3×10^{2}	≈ 0.4	(6)
McKibben	0.2-0.3	≈ 4	1.5×10^{3}-1×10^{4}	-	(8)

[a)]DE actuators demonstrate extensional strain up to 380%.[7] We have converted all actuation strains in this table to contractile strain (a value always less than 1) for a fair comparison.

Supporting Movie Legends

Movie S1. A VAMP fabricated in Ecoflex (E = 43 kPa) lifting a 20 g weight. The inside of the membrane is painted with a black marker to reveal the shape of the chamber more clearly. A black outline is visible after the actuator contracts.

Movie S2. A VAMP fabricated in Elastosil (E = 520 kPa) lifting a 500 g weight. The shape of the chambers is revealed after contraction as the membrane buckles inward and generates a shadow.

Movie S3. A VAMP fabricated in 3D-printed urethane rubber (E ≈ 2.5 MPa) lifting a 2 kg weight.

Movie S4. A VAMP actuating an "arm-like" structure, with mechanics similar to that employed by a human bicep muscle. It takes the arm 0.5 s to complete the contractile motion, although this VAMP is not optimized for speed.

Movie S5. A VAMP actuating an "arm-like" structure that lifts a volleyball, which has a standard size and weighs 274 g. It takes the arm 0.6 s to complete the contractile motion. This VAMP is also not optimized for speed.

Movie S6. A human arm of a young male researcher contracting as rapidly as possible. It takes the arm 0.17 s to complete the contractile motion.

Movie S7. A human arm of a young male researcher contracting as rapidly as possible, while lifting a volleyball, which has a standard size and weighs 274 g. It takes the arm 0.2 s to complete the contractile motion.

Movie S8. The "arm-like" structure flipping over a cup in its hand.

Movie S9. The "arm-like" structure throwing and catching a balloon in its hand.

Movie S10. The "arm-like" structure throwing a ball into a cup without knocking over the cup.

Movie S11. A VAMP preserves its contractile function even after being punctured by a cannula 2 mm in diameter.

Movie S12. The VAMP used in the "arm-like" structure lifting a 500 g weight. We also recorded this actuation using a high-speed camera to perform dynamic characterization.